BENCHMARKING OF THE RAPID TOOL FOR A SUBCRITICAL FACILITY

Nathan J. Roskoff and Alireza Haghighat*
Nuclear Engineering Program
Department Of Mechanical Engineering
Virginia Tech
900 N. Glebe Road, Arlington, VA, USA, 22203
roskofnj@vt.edu; haghighat@vt.edu

Marshall Millett and Joe Leidig
Mechanical Engineering Department
United States Naval Academy
590 Holloway Road, Annapolis, MD, USA, 21402
millett@usna.edu; leidig@usna.edu

ABSTRACT

The RAPID (Real-time Analysis for Particle transport and In-situ Detection) tool is benchmarked using the U.S. Naval Academy's subcritical reactor (USNA-SCR) facility. RAPID is a tool capable of real-time calculation of the system eigenvalue, subcritical multiplication, axially-dependent, pin-wise, fission distribution, and determination of detector responses. RAPID utilizes a Multi-stage Response-function Transport (MRT) approach using the Fission Matrix method to perform fixed-source, eigenvalue, and subcritical multiplication calculations and the adjoint function methodology to calculate detector responses. RAPID is enabled to do real-time calculations by utilizing databases of pre-calculated response coefficients. RAPID's real-time calculation capability is particularly important for nuclear materials monitoring and safeguards applications. The USNA-SCR contains 268 annular natural uranium fuel rods, arranged in a hexagonal lattice, placed in a tank of water. The USNA-SCR is driven by a PuBe source located at the center of the fuel bundle. The neutron measurements were performed with a ^{3}He proportional counter within the annulus of the fuel pins. The set of measurements include cross-core radial slices at fixed axial positions. Measured detector responses are compared with calculated reaction rates of a fixed-source MCNP Monte Carlo calculation. RAPID calculations are performed for eigenvalue calculations and it's results are compared with a reference MCNP Monte Carlo calculation.

Key Words: fission matrix, benchmark, subcritical

1 INTRODUCTION

The RAPID (Real-time Analysis for Particle transport and In-situ Detection) code system is based on the MRT (Multi-stage Response-function Transport) approach [1] for solving complex radiation transport problems in real-time. The foundation of an MRT approach is to partition the problem into several stages, each of which can be represented by a response function or a set

*www.nsel.ncr.vt.edu

of coefficients. These individual stages are then coupled through a set of linear equations which are solved iteratively using sets of pre-calculated response functions or coefficients. Typically, these response functions/coefficients are compiled into a database covering a range of variables. This allows a user to calculate system responses on-the-fly, without the need for any further computationally intensive transport calculations.

RAPID pre-calculates Fission Matrix (FM) coefficients for determination of system eigenvalue, subcritical multiplication, and pin-wise axial fission densities. RAPID has been previously demonstrated to accurately calculate these quantities for spent fuel pools (SFP) [2–4] and for storage casks [5]. Additionally, unlike the standard, brute force Monte Carlo approach for solving eigenvalue problems, RAPID does not suffer from issues of under sampling and source convergence for loosely coupled problems such as SFP's [6].

This paper discusses the benchmarking of RAPID based on the U.S. Naval Academy Subcritical Reactor (USNA-SCR). The geometry and materials of the USNA-SCR are presented and the experimental setup. In addition to the RAPID calculations, a reference MCNP5 [7] calculation is performed.

Section 2 will present the RAPID MRT technique. Section 3 will define the USNA-SCR facility and describe the experimental setup. Section 4 provides the results of a detailed MCNP analysis of the USNA-SCR, a comparison of calculated and experimental detector responses, and a comparison of RAPID results with those from the MCNP model of the USNA-SCR.

2 RAPID METHODOLOGY

The RAPID code system comprises the following stages: (1) burnup calculations to determine fuel isotopics and neutron spectra using the SCALE/TRITON [8], (2) evaluation of FM coefficients via fixed-source MCNP calculations, (3) solution of the FM equations for k-effective, subcritical multiplication, and fission densities, and (4) coupling fission densities with an importance function to calculate detector responses via the adjoint function methodology [9]. Note that Stages 1 and 4 are not pertinent to this paper and will not be discussed.

2.1 Fission Matrix Method

The FM method [10] can take two forms, depending on the type of problem. For a sub-critical multiplication problem, in which the fission source is driven by an independent source in the spent fuel (i.e., spontaneous fission and (α, n) reactions), the induced fission source in cell i is given by Equation (1)

$$F_i = \sum_{j=1}^{N} (a_{i,j} F_j + b_{i,j} S_j), \tag{1}$$

where F_j is the induced fission source strength in fuel pin j, S_j is the intrinsic (or independent) source strength in fuel pin j, $a_{i,j}$ is the number of fission neutrons directly produced in fuel pin i due to a fission neutron born in fuel pin j, and $b_{i,j}$ is the same as $a_{i,j}$ except for intrinsic source neutrons.

These values are different because S and F should have different spatial and energy distributions within each cell. N is the total number of computational cells.

We also consider the eigenvalue problem, as in Eq. (2)

$$F_i = \frac{1}{k} \sum_{j=1}^{N} a_{i,j} F_j, \tag{2}$$

where k is the system eigenvalue.

The fission matrix method results in a set of N linear equations, which can be solved for F and k given the $a_{i,j}$ coefficients. The main difficulty is how to calculate the coefficients, and to decide on a computational cell size that is small enough to give detailed and accurate results, but not so large that the linear system becomes intractable. This can happen quickly as the matrix is of size $N \cdot N$.

2.2 FM Coefficient Generation

To utilize the FM methodology in real-time it is necessary to pre-calculate the FM coefficients ($a_{i,j}$). To calculate the FM coefficients a series of fixed-source MCNP calculations are performed, with the source located in one of each of the computational cells (location i). In our case, a computational cell is a 1/4" axial segment of a single fuel pin. The total fission neutron production rate, i.e. $\int dV \nu \Sigma_f \phi$, is tallied in all surrounding pins for all axial levels (location j). The tally results from all independent fixed-source calculations are compiled to create the FM coefficient $a_{i,j}$. Once the FM coefficients have been calculated, there is no more need for detailed transport calculations.

3 DESCRIPTION OF THE USNA-SCR FACILITY

This section will describe the geometry and materials of the USNA-SCR facility and the experimental setup.

3.1 USNA Subcritical Reactor (USNA-SCR)

The USNA-SCR facility is a pool-style subcritical reactor with natural uranium fuel and light water moderator. The pool is an open top, aluminum cylindrical vessel wrapped by borated foam. There are a total of 268 fuel rods are arranged in a hexagonal lattice (note that there are 3 missing rods on the right-hand side of the fuel bundle), shown in Figure 1a. The fuel rods are constructed of hollow aluminum tubes containing 5 annular fuel slugs which are surrounded by air (they are open at the top). At the bottom of each fuel rod there is a hollow acrylic tube which elevates the fuel from the bottom of the pool. Neutrons are injected into the system via a plutonium beryllium, PuBe, (α,n) source. The PuBe material is contained in a stainless steel capsule that is positioned within an aluminum tube in the central location of the fuel assembly. The source capsule is elevated from the bottom of the tube by a small stand, as shown in Figure 1b.

The pool outer diameter is 121.29 cm with a thickness of 0.64 cm and a height of 152.40 cm. The water depth is 135.66 cm. The borated foam thickness is 0.79 cm. The fuel rod tube outer diameter

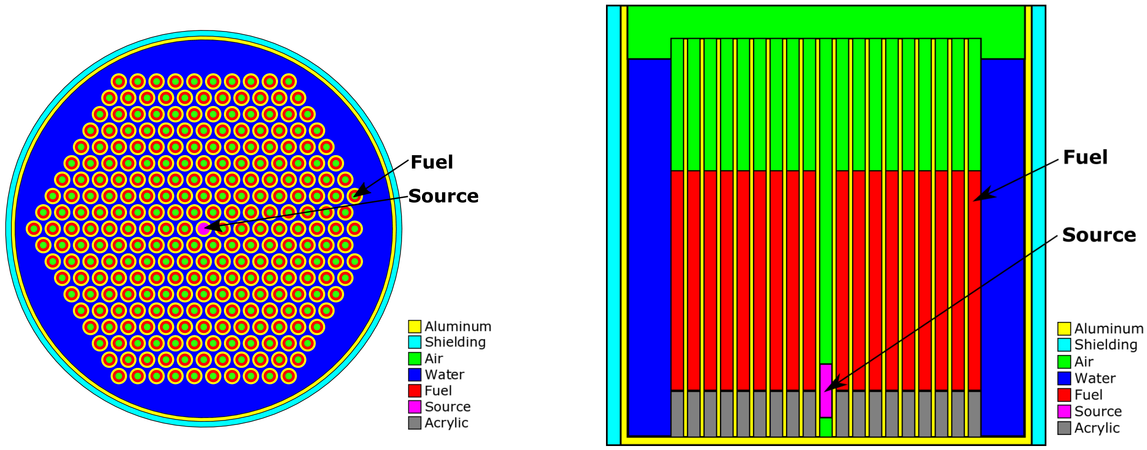

(a) Top view (x-y plane). **(b) Side view (y-z plane).**

Figure 1. Geometry of the USNA-SCR (not drawn to scale).

is 3.45 cm with a thickness of 0.18 cm and a height of 139.70 cm. The fuel rod pitch is 4.81 cm. The fuel slug outer diameter is 3.05 cm with an inner diameter of 1.27 cm and total height of 104.14 cm. The fuel is elevated 15.24 cm from the bottom of the rods. The source capsule outer diameter is 3.02 cm with a total height of 25.30 cm; the PuBe slug (within the capsule) has a diameter of 2.55 cm, height of 18.5 cm, and is axially centered within the capsule. The source capsule is elevated 5.00 cm from the bottom of the rod.

The source material composition is not explicitly known, but the ratio of plutonium to beryllium is assumed to be 1:13, i.e., $PuBe_{13}$ [11]. Additionally, due to the age of the source, the buildup of americium as a consequence of the beta decay of ^{241}Pu is considered. The source spectrum has been calculated using the SOURCES-4C [12] code for an assumed material composition obtained from the DOE 2013 Standard [13]. Figure 2 shows the neutron source spectrum calculated by SOURCES-4C.

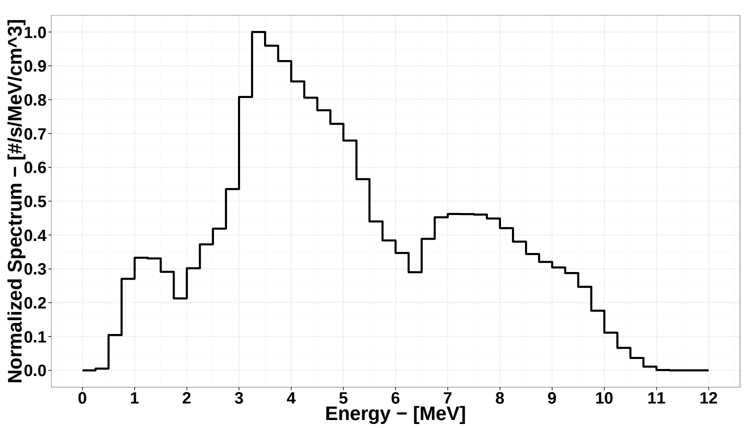

Figure 2. PuBe source spectrum.

Figure 2 shows that the most probable neutron energy is within 3.00 - 3.25 MeV. The average neutron energy is calculated to be 4.84 MeV and the source strength is 2.32 $\times 10^6$ n/s/cm^3.

3.2 Experimental Setup

A set of in-core neutron measurements were performed along three axes labeled 11, 12, and 13, as shown in Figure 3. For this, a stainless steel constructed, cylindrical LND, Inc. ^{3}He proportional neutron detector [14] was positioned at a fixed axial height within the annulus of the fuel slugs. The effective detector height is 28.7 mm, the diameter 9.65 mm, and the gas is held at an absolute pressure of 3040 torr, i.e., 4 times standard atmospheric pressure. The bottom of the detector volume was elevated 27.18 cm from the bottom of the fuel tubes.

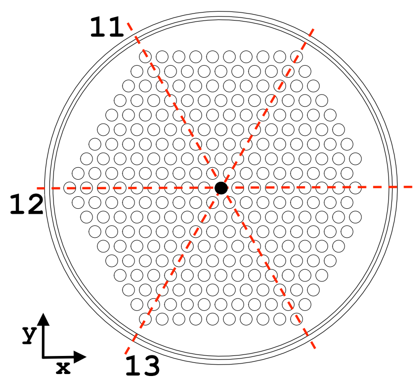

Figure 3. The three axes (11,12, and 13) for in-core neutron measurements. The black dot indicates the source location.

4 RESULTS

A fixed-source MCNP Monte Carlo calculation is analyzed and calculated ^{3}He reaction rates are compared to measured detector responses. A RAPID eigenvalue calculation is performed and results are compared to an MCNP reference calculation.

4.1 MCNP Calculation Results

Using the SCALE 238-group structure [15], an energy-dependent neutron flux tally was obtained and a volume-average neutron spectrum was calculated for the USNA-SCR, as shown in Figure 4. This figure indicates that the most probable neutron energy of this system is $\approx$0.03 eV.

The neutron flux distribution throughout the core was calculated using a superimposed MCNP mesh tally with tally bin dimensions of 1.22 cm$\times$1.22 cm$\times$1.58 cm (x, y, and z, respectively). Figure 5 shows energy-integrated radial flux, at x=0 cm and z=-102cm (through source axial center-line), and an axial flux, at x=0 cm and y=0 cm (through source radial center-line).

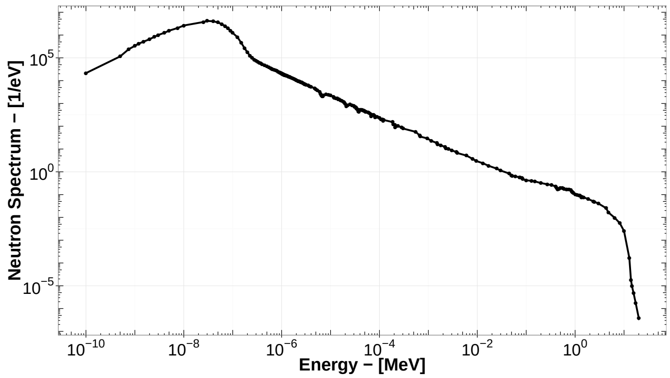

Figure 4. USNA-SCR 238-group neutron spectrum (maximum relative uncertainty 1.93% in group 238).

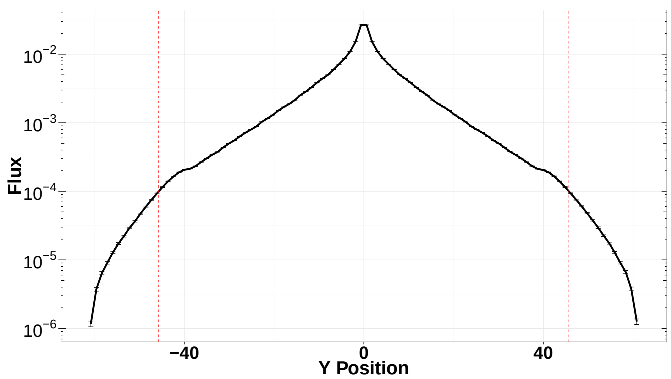

(a) Radial profile (maximum relative uncertainty 4.83%). Red lines indicate edge of fuel bundle.

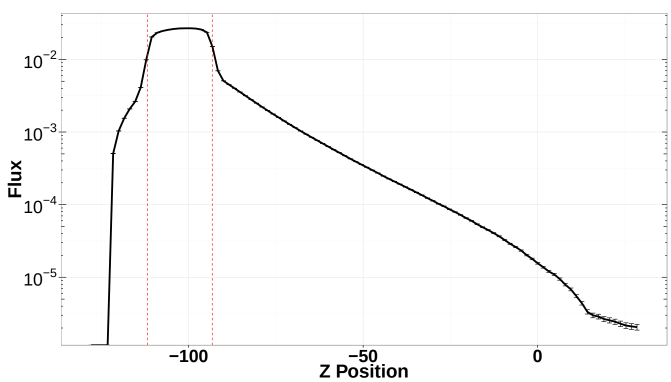

(b) Axial profile (maximum relative uncertainty 4.60%). Red lines indicate bottom/top of source.

Figure 5. MCNP calculated flux distribution of the USNA-SCR. Error bars represent 2σ uncertainties.

Additionally, a multi-group mesh tally was obtained considering the SCALE 49-group structure [15]. Figure 6 shows the spatial flux distribution in Group 49 (1.0E-11 < E < 3.0E-9 MeV) which includes the average neutron energy. The thermal (E < 3.0E-9 MeV) flux distribution, Figure 6, demonstrates the expected physical behavior of the flux peaking locally in the moderator regions (water) and is locally minimized in the fuel regions. The thermal flux drops nearly an order of magnitude between

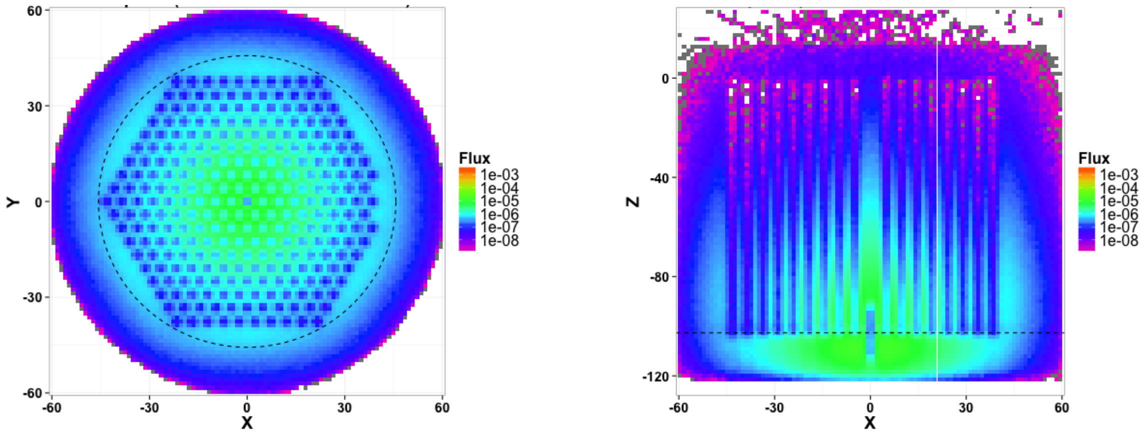

(a) X-Y view. **(b) X-Z view.**

Figure 6. USNA-SCR flux distribution for Group 49 (1.0E-11 < E < 3.0E-9 MeV), includes the average neutron energy. Note that tallies with a zero value are not plotted.

these material regions. The thermal flux drops by nearly three orders of magnitude when moving axially from the source to the top of the fuel rods (Figure 6b).

Figure 7 shows the spatial flux distribution in Group 4 (3.0 < E < 4.8 MeV) which includes the most probable neutron energy of the PuBe source. The fast flux distribution, Figure 7, demonstrates that

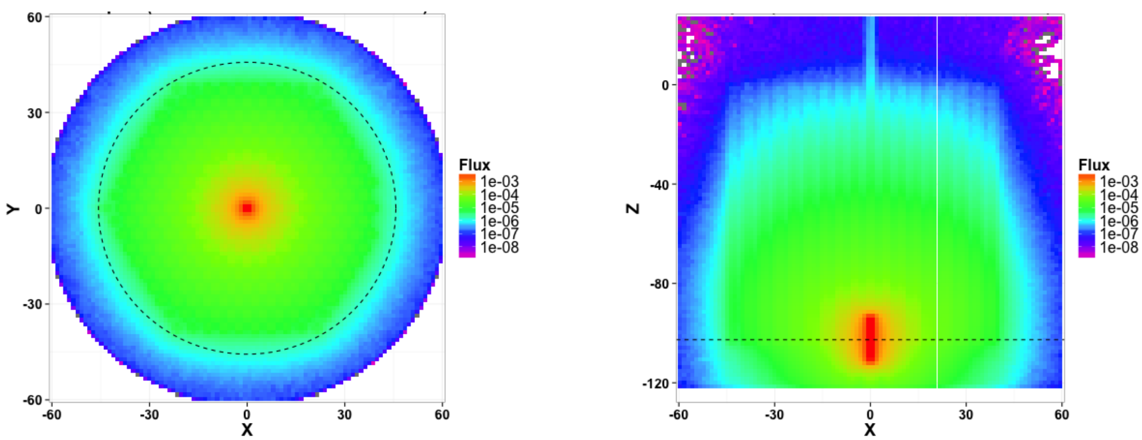

(a) X-Y view. **(b) X-Z view.**

Figure 7. USNA-SCR flux distribution for Group 4 (3.0 < E < 4.8 MeV) - includes PuBe source peak energy. Note that tallies with a zero value are not plotted.

the fast flux is clearly peaked within the PuBe source region and drops by an order of magnitude when moving away radially 15cm, after which it remains fairly constant within the fuel region (Figure 7a). After the fuel region the flux drops another three orders of magnitude. Axially the flux drops an order of magnitude shortly past the top/bottom of the source region, then remains relatively constant up to z=-40cm within the fuel region. After this point, the flux drops about 2 orders of magnitude to the top of the fuel region, and then drops another two orders of magnitude to the top of the of the pool.

4.2 Comparison of Experimental and Calculated Detector Responses

The MCNP model of the USNA-SCR was used to calculate the expected detector response within the active detector volume for each radial slice, as in Figure 3. The calculated detector response was obtained by calculating the ^{3}He absorption reaction rate in the detector volume, i.e. $\int dV_{det.}\Sigma_{a,^3He}\phi$. Figure 8 shows the ratio of calculated reaction rate response to measured detector response (C/E) measurement for the three experimental axes. The error bars represent a combined uncertainty which includes the statistical uncertainty from the MCNP calculation and the counting uncertainty of the measurements. This figure shows that the calculated detector responses are in very good

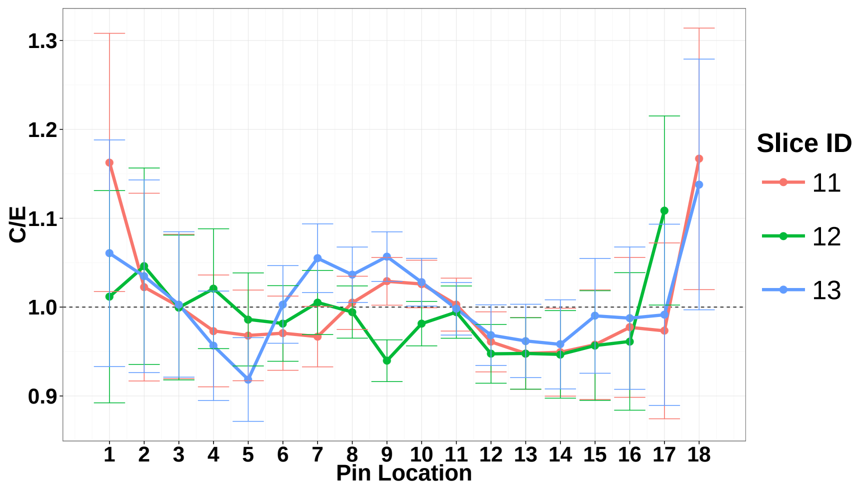

Figure 8. Calculated detector response vs. experimental measurement ratio for the 3 radial profiles.

agreement with the measured detector responses. Results compare very well (+/- 10%) except for the boundary locations which are ≈5% higher. The observed larger C/E values at the boundaries are attributed to the higher counting uncertainty in the measurements. Additionally, note that Pin Location 9 for Slice 12 (green) and Pin Location 5 for Slice 13 (blue) show a slight deviation from the expected behavior. The cause of this deviation is related to the measurements and is being investigated.

4.3 Comparison of RAPID Results with MCNP Model

The MCNP model used above for comparison of calculated vs. experimental detector responses is used to calculate the k-effective and pin-wise axially dependent fission densities of the USNA-SCR. Table I shows a comparison of the calculated system k-effective from MCNP and RAPID. This table shows that the RAPID calculated k-effective agrees reasonably well with MCNP calculated results.

Table II shows the required computation time for both calculations. This table shows that the RAPID's serial calculation, i.e. 1 processor, is significantly faster than the MCNP calculation using 8 processors.

Table I. Comparison of calculated eigenvalues.

Code	k	Rel. Diff. [pcm]
MCNP	0.87278 (±3pcm)	—
RAPID	0.87420	163

Table II. Computation time (wall-clock) for RAPID and MCNP reference calculation.

Code	No. of Processors	Time [min]	Speedup
MCNP	8	819.50	—
RAPID	1	0.22	3774

Figure 9 compares the integrated (in x-y and y-z), normalized fission densities for the two calculation methods. Figure 9a shows the axial behavior (integrated in x-y), and Figure 9b shows the radial behavior (integrated in y-z). These results indicate that the RAPID calculated fission density is in

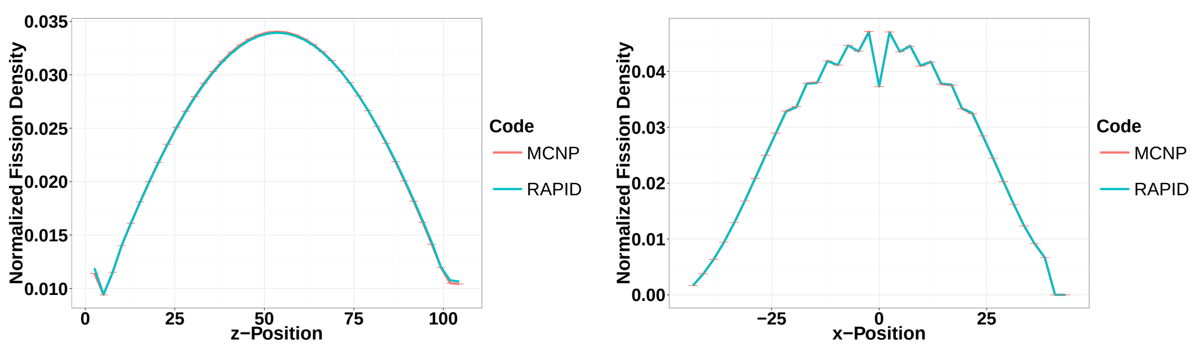

(a) Profile along z direction (integrated in x and y directions). **(b) Profile along x direction (integrated in y and z directions).**

Figure 9. Integrated normalized fission density calculated by RAPID and MCNP. Error bars represent 2σ uncertainty, maximum relative uncertainty of MCNP fission density tally is 1.13%

good agreement with the MCNP calculated values. The relative differences of RAPID calculated fission densities compared with the MCNP reference solution are within +/- 4%.

5 CONCLUSIONS AND FUTURE WORK

We have benchmarked RAPID on the USNA-SCR experimental facility and also obtained a reference solution using MCNP. RAPID, MCNP, and measured detector responses are all in good agreement. In attempt to develop a qualified benchmark problem we intend to collect further experimental data and perform sensitivity and uncertainty analysis. In addition, we intend to perform further sensitivity analysis on the FM coefficient generation techniques.

6 REFERENCES

[1] A. Haghighat, K. Royston, and W. Walters, "MRT methodologies for real-time simulation of nonproliferation and safeguards problems," *Annals of Nuclear Energy*, **87**, pp. 61–67 (2016).

[2] W. Walters, N. Roskoff, and A. Haghighat, "A Fission Matrix Approach to Calculate Pin-wise 3-D Fission Density Distribtuion," *Joint International Conference on Mathematics and Computation (M&C), Supercomuting in Nuclear Applications (SNA) and the Monte Carlo (MC) Method*, La Grange Park, Illinois, April 19-23, 2015, American Nuclear Society.

[3] W. Walters, N. Roskoff, and A. Haghighat, "Use of the Fission Matrix Method for Solution of the Eigenvalue Problem in a Spent Fuel Pool," *PHYSOR 2014 - The Role of Reactor Physics toward a Sustainable Future*, Kyoto, Japan, September 28 - October 3, 2014.

[4] N. Roskoff, A. Haghighat, and V. Mascolino, "Analysis of RAPID Accuracy for a Spent Fuel Pool with Variable Burnups and Cooling Times," *Proceedings of Advances in Nuclear Nonproliferation Technology and Policy Conference*, Santa Fe, NM, September 25-30, 2016.

[5] V. Mascolino, A. Haghighat, , and N. Roskoff, "Evaluation of RAPID for a UNF Cask Benchmark Problem," *Proceedings of ICRS-13 & RPSD-2016*, Paris, France, October 3-6, 2016.

[6] M. Wenner and A. Haghighat, "A Fission Matrix Based Methodology for Achieving an Unbiased Solution for Eigenvalue Monte Carlo Simulations," *Progress in Nuclear Science and Technology*, **2**, pp. 886–892 (2011).

[7] X-5 Monte Carlo Team, "MCNP-A General Monte Carlo N-Particle Transport Code, Version 5," Los Alamos National Laboratory (2005).

[8] "SCALE: A Comprehenisve Modeling and Simulation Suite for Nuclear Safety Analysis and Design," Oak Ridge National Laboratory (2011).

[9] G. Bell and S. Glasstone, *Nuclear Reactor Theory*, Krieger Publish Company (1970).

[10] A. Haghighat, *Monte Carlo Methods for Particle Transport*, CRC Press, Taylor & Francis Group, Boca Raton, FL (2015).

[11] M. Anderson and R. Neff, "Neutron energy spectra of different size 239 PuBe (α, n) sources," *Nuclear instruments and Methods*, **99**, *2*, pp. 231–235 (1972).

[12] E. Shores, "SOURCES 4C: A Code for Calculating (, n), Spontaneous Fission, and Delayed Neutron Sources and Spectra," LA-UR-02-1839 (2002).

[13] DOE Standard, "3013-2000" Stabilization," *Packaging, and Storage of Plutonium-Bearing Materials* (2000).

[14] "250 Cylindrical He-3 Neutron Detector," LND, Inc. (2016).

[15] W. Jordan, S. Bowman, and D. Hollenbach, "SCALE cross-section libraries," *Vol. III, Sect. M4 of SCALE: A Modular Code System for Performing Standardized Computer Analysis for Licensing Evaluation, NUREG/CR-0200, Rev*, **7**, *3* (1997).